Likely role of promoter reconstitution in Mpr-mediated D29 resistance by *Mycobacterium smegmatis*

Buhari Yusuf, [1,2,3,4] Yanan Ju, [1,2,3,5] Biao Zhou, [6] Abdul Malik, [1,2,3,4] Md Shah Alam, [1,2,3,4] Lijie Li, [1,2,3,5] Haftay Abraha Tadesse, [1,2,3,4] Belachew Aweke Mulu, [1,2,3,4] Cuiting Fang, [1,2,3,7,8,9] Xirong Tian, [1,2,3,7,9] Hongyi Chen[10], Li Wan,[1,2,3] , Liqiang Feng,[1,2,3] Xiaoli Xiong[1,2,3,8,9], Shuai Wang, [1,2,3] Tianyu Zhang [1,2,3,7,8,9]

[1] State Key Laboratory of Respiratory Disease, Guangzhou Institutes of Biomedicine and Health, Chinese Academy of Sciences, Guangzhou 510530, China

[2] China-New Zealand Joint Laboratory on Biomedicine and Health, Guangzhou Institutes of Biomedicine and Health, Chinese Academy of Sciences, Guangzhou 510530, China

[3] Guangdong-Hong Kong-Macao Joint Laboratory of Respiratory Infectious Diseases, Guangzhou Institutes of Biomedicine and Health, Chinese Academy of Sciences, Guangzhou 510530, China

[4] University of Chinese Academy of Sciences, Beijing 100049, China

[5] School of Life Sciences, University of Science and Technology of China, Hefei 230027, China

[6] State Key Laboratory of Respiratory Disease, Guangzhou Chest Hospital, Institute of Tuberculosis, Guangzhou Medical University, Guangzhou 510095, China

[7] Guangzhou Medical University-Guangzhou Institutes of Biomedicine and Health Joint School of Life Sciences, Guangzhou Medical University, Guangzhou 511436, China

[8] State Key Laboratory of Respiratory Disease, Guangzhou Chest Hospital, Guangzhou, China

[9] Guangzhou National Laboratory, Guangzhou 510005, China

[10] West China School of Public Health, Sichuan University, Chengdu 610041, China

Correspondence: Tianyu Zhang, zhang_tianyu@gibh.ac.cn

Abstract

The multi-copy phage resistance gene (*mpr*) of *M. smegmatis* is a major factor in resistance to the lytic mycobacteriophage D29. Mpr is a membrane-bound exonuclease that cleaves phage DNA post injection, hence blocking downstream stages in the phage infection cycle. The mechanism of resistance allows for adsorption, is non-abortive and independent of any mutation in the gene. Rather, it depends on overexpression of a wild type copy of the gene. However, the underlying factor behind *mpr* overexpression in spontaneous D29-resistant mutants of *M. smegmatis* remained elusive. Here, we report that D29 infection triggers insertion sequence (IS) rearrangements, including the transposition and integration of IS6120 directly upstream of *mpr*. Mutants with IS6120 integration upstream of *mpr* show highly elevated Mpr expression. Whole genome sequence analysis reveals that IS6120 introduced a putative transcription factor-binding site and a canonical -35 promoter element at the integration site, hence reconstituting a fuller promoter (*rcp*) than the original promoter (*wtp*) at the site. Promoter reporter assays suggest that *rcp* is a far stronger promoter than *wtp*, implying that elevated *mpr* expression in D29-resistant mutants with this transposition event could be due to promoter reconstitution. While strains with this transposition event appear to grow normally, *rcp*-driven, vector-borne Mpr overexpression appears to be toxic as it barely allows for colony formation on agar plates. This study reports a previously unknown factor likely behind *mpr* regulation in *M. smegmatis*, adding to the existing knowledge of mycobacterial anti-phage defense mechanisms and guiding rational phage engineering efforts for therapeutic applications.

Keywords: *Mycobacterium smegmatis*, mycobacteriophage D29, promoter reconstitution, Mpr, phage resistance.

54 **Introduction**

55 Antimicrobial resistance (AMR) remains a serious public health threat, and despite efforts to
56 develop novel therapeutics or vaccines, the threat remains ever existent. This is because the pace
57 at which bacterial pathogens develop resistance to antimicrobials surpasses the rate at which new
58 therapeutics are introduced into clinical use. Conventional antibiotic treatments occasionally fail
59 due to extensive drug resistance, hence complicating disease management. In fact, it is estimated
60 that global death toll due to bacterial AMR may surpass 39 million between 2025 and 2050 (1).
61 For this reason, interest in phage therapy as an alternative to conventional antibiotic therapy is
62 gaining significant traction.

63 Phage therapy is the use of bacteria-eating viruses (or bacteriophages) to treat bacterial infections.
64 Bacteriophages are highly specific, relatively safe and hold significant potential as alternatives to
65 redundant, toxic antibiotic therapy. Currently, phage therapy is only available to patients under
66 the framework of compassionate use (2). Compassionate use of phage therapy against drug-
67 resistant mycobacterial infections have further highlighted the significant potential of phage
68 therapy even in complicated cases of failed antibiotic therapy (3–9). However, bacterial
69 pathogens can develop resistance to bacteriophages, which represents a potent threat to
70 sustainable utility of phage therapy.

71 Bacterial pathogens have evolved an extensive arsenal of anti-phage defense systems, including
72 clinical bacterial isolates (10–13). The lytic mycobacteriophage D29 has demonstrated
73 therapeutic potential in compassionate use against BCG and *Mycobacterium abscessus* infections
74 (5,7). However, a resistance mechanism against D29 and its parent L5 already exists in the
75 model bacterium *Mycobacterium smegmatis* (14). The multicopy phage resistance gene (*mpr*) of
76 *M. smegmatis* is a major factor in D29 resistance. Mpr is a membrane-bound exonuclease that
77 mediates resistance via cleavage of phage DNA post injection, which blocks downstream stages
78 of the phage lifecycle and inhibit phage propagation (15). Mpr contains a domain of unknown
79 function (DUF4352) that is believed to be of viral origin, suggesting that *M. smegmatis* obtained
80 this protein during the course of its evolution with viral predators and repurposed it for anti-
81 phage defense (16). The protein has also been reported to aid non-homologous end joining
82 (NHEJ)-mediated anti-phage defense in *M. smegmatis* (17), further highlighting its relevance to
83 antiviral defense. However, the role of Mpr in D29 resistance is independent of any genetic

84 change in the gene, but rather depends on overexpression of a wild type copy of the gene. The
85 exact factor behind elevated Mpr expression in spontaneous D29-resistant mutants remained
86 unknown.

87 We report here that infection with D29 triggers IS rearrangements in *M. smegmatis*, including the
88 transposition and integration of IS6120 directly upstream of *mpr*. IS6120 introduces a canonical -
89 35 promoter element as well as a putative transcription factor-binding site (TFBS) for leucine-
90 responsive regulatory protein (Lrp), hence reconstituting a fuller promoter than the original
91 promoter at the integration site. Promoter reporter assays show that the reconstituted promoter
92 (*rcp*) is far stronger than the wild type promoter (*wtp*), which could represent a previously
93 unknown regulatory mechanism for the toxic protein Mpr in *M. smegmatis*.

94

95

96

97

98

99

100

101

102

103

104

105

106

107

108

Materials and Methods

Bacterial strains, phage and growth conditions

Cloning experiments were carried out in *E. coli* Trans1 (TransGen Biotech., China). *E. coli* was maintained in liquid or on solid Luria-Bertani medium. Selective growth of *E. coli* was carried out in the presence of kanamycin (kan, 50 μg/mL), ampicillin (amp, 100 μg/mL) or zeocin (zeo, 30 μg/mL). *M. smegmatis* mc^2 155 was maintained in Middlebrook 7H9 (Difco) medium supplemented 10% OADC, 0.2 % glycerol and 0.05% Tween 80. *M. smegmatis* was selectively grown in liquid or on solid medium in the presence of the following concentrations of antibiotics: kan (liquid, 20 μg/mL; solid, 50 μg/mL); zeo (30 μg/mL). All liquid cultures were maintained at 37 ^{o}C with shaking at 200 revolutions per minute (rpm). The phage used in this study is the lytic mycobacteriophage D29. All D29 infection experiments were carried out at 37 ^{o}C in the presence of 2 mM $CaCl_2$.

Phage amplification

Wild type *M. smegmatis* (Ms^{Wt}) was grown in 7H9 medium to OD_{600} 0.8-1 at 37 ^{o}C with shaking. The cells were pelleted and washed thrice in MP buffer, then re-suspended in 1.5 mL of the same buffer. Ten-fold serial dilutions of the phage stock were prepared in MP buffer until 10^{-4} dilution factor. A four-component mixture was prepared by adding top agar, washed Ms^{Wt} cells, D29 at 10^{-4} dilution and $CaCl_2$ at a final concentration of 2 mM. The mixture was mixed by pipetting and poured into plain 7H10 plates, spread evenly, allowed to dry and incubated at 37 ^{o}C for 12-24 hours. This was followed by addition of 2.5 mL of sterile MP buffer into each plate and rocking on an orbital shaker at room temperature for 4-5 hours. The MP buffer was then recovered from the plates by pipetting, centrifuged at 3,500 ×g for 10 minutes, then passing the supernatant through a 0.22 μm filter. The filtrate containing the amplified phage was stored at 4 ^{o}C.

Generation of spontaneous D29-resistant strains

Spontaneous D29-resistant strains were generated by subjecting Ms^{Wt} to four sequential rounds of extended exposures to mycobacteriophage D29 to increase the chance of retaining resistant clones and eliminating susceptible ones (18,19). In the first exposure cycle, bacterial cells were grown to OD_{600} 1.0, washed three times in MP buffer and re-suspended in 1 mL of MP buffer,

138 infected with D29 and incubated at 37 ºC for 7 hours with regular shaking. Cells from the 7-hour
139 incubation were collected by centrifugation at 13,000 ×g for 3 minutes, washed three times in
140 PBS-Tween 80, and re-suspended in 1 mL of the same medium. 50 uL of the washed cells were
141 sub-cultured in 7H9 medium containing 0.05 % Tween 80 until OD_{600} 1.0. This resulting culture
142 was washed three times in MP buffer, infected with D29 and incubated at 37 ºC for 14 hours
143 with regular shaking. This continued until the fourth exposure cycle, with the incubation period
144 extended by 7 hours after the previous exposure cycle (21 and 28 hours for third and fourth
145 exposure cycles, respectively). For every infection cycle, MP buffer was used as the medium of
146 infection, bacterial cells were infected at MOI of 5, and it was ensured that $CaCl_2$ was added to a
147 final concentration of 2 mM. After the final 28-hour exposure, the cells were collected by
148 centrifugation, washed in PBS-Tween 80, diluted and plated to collect single colonies.

149 **Phage susceptibility testing (PST)**

150 Phage susceptibility testing was carried out by plaque and spot-kill assays as well as on D29-
151 seeded 7H10 plates. Bacterial cells were grown in 7H9 medium to OD_{600} 0.8-1. The grown cells
152 were pelleted by centrifugation at 3,500 ×g for 10 minutes. The supernatant was discarded and
153 the pellet was washed three times in MP buffer and re-suspended in 0.5-1 mL of the same buffer.
154 Ten-fold serial dilutions of D29 were prepared. For plaque assay, a soft overlay of top agar,
155 phage, bacterial cells and 2 mM $CaCl_2$ was prepared and poured into plain 7H10 plates in
156 triplicates. The plates were dried and incubated at 37 ºC for 12-24 hours before enumeration of
157 plaque forming units. For spot-kill assay, a soft overlay of top agar, bacterial cells and $CaCl_2$ was
158 poured into a 7H10 plate, spread evenly and allowed to dry. Two microliters of ten-fold serial
159 dilutions of the phage were spotted on the dried soft overlay, allowed to dry, and incubated at 37
160 ºC for 12-24 hours. For PST on phage-seeded plates, 2 µL of ten-fold serial dilutions of the
161 bacteria was spotted on 7H10 plate seeded with 10^7 – 10^9 plaque forming units per milliliter
162 (PFU/mL) of D29, allowed to dry, and incubated at 37 ºC for 3-5 days. Serial dilution of the
163 bacteria was carried out in MP buffer containing 2 mM $CaCl_2$, and 7H10 plate containing no
164 phage was used as a negative control.

165 **Phage adsorption assay**

166 Phage adsorption assay was carried out as described previously (19,20). Bacterial cells were
167 grown to mid log phase, washed three times and re-suspended in MP buffer. The cells were

168 diluted in MP buffer to OD_{600} 0.3. Ten-fold serial dilutions of D29 were prepared in MP buffer
169 until 10^{-3}. To determine terminal phage adsorption, 30 μL of 10^{-3} dilution of the phage was added
170 to 200 μL aliquot of diluted bacteria, and $CaCl_2$ was added to a final concentration of 2 mM. The
171 mixture was incubated at 37 °C with shaking for 60 minutes. Simultaneously, same quantity of
172 same phage inoculum was added to 200 μL of sterile MP buffer, 2 mM $CaCl_2$ was added, mixed,
173 and immediately centrifuged at 5000 ×g for 3 minutes. The supernatant was collected, diluted
174 and used for plaque assay on MP buffer-washed Ms^{Wt}. After the 60 minutes shaking of phage-
175 bacteria mixture, the mixture was also centrifuged at 5000 ×g for 3 minutes, the supernatant was
176 collected, diluted and used for plaque assay on MP buffer-washed Ms^{Wt}. Plates were allowed to
177 dry, incubated at 37 °C for 24 hours before enumeration of plaque forming units. Plates were
178 prepared in triplicates, and data was presented as percentage of adsorbed phage. For
179 determination of phage adsorption rates, same phage-bacteria mixtures and incubation conditions
180 were prepared for plaque assay at 0-, 30- and 60-minute time points. Collected data was
181 presented as percentage of unadsorbed phage.

182 **Colony morphology and spot inhibition by kanamycin and zeocin**

183 All strains were grown in 7H9 medium to OD_{600} 0.8-1 and diluted to OD_{600} 0.6. Two microliters
184 from diluted culture of each strain was spotted on plain 7H10 plate and allowed to dry. For
185 susceptibility testing to kan (50 μg/mL) or zeo (30 μg/mL), the cells were spotted on 7H10 plates
186 containing indicated concentration of either drug. Dried plates were incubated at 37 °C for 3-4
187 days.

188 **Whole genome sequencing (WGS)**

189 Genomic DNA (gDNA) extraction and sequencing were carried out by Shanghai Jingnuo
190 Biotechnology Co., Ltd. (Shanghai, China). A modified Cetyltrimethylammonium bromide
191 (CTAB) method was used for extraction of gDNA (21). Extracted gDNA was quantified using
192 Qubit 2.0 Fluorometer (ThermoFisher, USA), followed by library construction using Hieff NGS®
193 OnePot Flash DNA Library Prep Kit (Yeasen, China) by enzymatic fragmentation of gDNA, end
194 repair, tail adenylation, adapter ligation, purification and PCR amplification. The library was
195 initially quantified using Qubit 2.0 and diluted. Fragment sizes were verified using Agilent 2100
196 bioanalyzer (Agilent, USA) and effective library concentration was quantified again by qPCR.

197 Libraries were pooled onto a flow cell, clustered using cBOT and sequenced using the NovaSeq
198 6000 high-throughput sequencing platform (Illumina, Inc., USA).

199 **Bioinformatics**

200 Next generation sequencing (NGS) data was analyzed on the GalaxyEU bioinformatics server
201 using default settings (22). Raw sequence reads were checked for quality using FASTQC (23),
202 and undesirable reads/reads of low quality were trimmed using FASTP (24). Mapping to the
203 reference genome (*M. smegmatis* mc^2 155, NCBI accession number CP000480.1) and variant
204 calling were achieved using Snippy (25), and the output data was exported as VCF and tab-
205 separated files. All detected variants were verified by Sanger sequencing.

206 **RNA extraction and RT-qPCR**

207 RNA extraction was carried out according to manufacturer instructions using Magen HiPure
208 Bacterial RNA Mini Kit (Magen, China). For bacterial growth to detect mRNA levels in the
209 presence and absence of D29 infection, the strains were first washed thrice in 7H9 medium
210 without Tween 80, sub-cultured in 7H9 (without Tween 80) containing 2 mM $CaCl_2$
211 with/without D29 at MOI 5. The strains were then washed thrice in PBS-Tween 80 prior to RNA
212 extraction. Extracted RNA was reverse transcribed using ExonScript All-in-One RT SuperMix
213 with DNase (EXONGEN, China) according to manufacturer instructions. The RT-qPCR reaction
214 was prepared and run according to manufacturer instructions using Taq Pro Universal SYBR
215 qPCR Master Mix (Vazyme Biotech., China). All reactions were run in C1000 Touch™ Thermal
216 Cycler (Bio-Rad, USA). SigA was used as control, and all wild type/untreated group expressions
217 were normalized to 1, and the treated/test group expression was presented as fold change.
218 Expression levels (fold) were represented as bar graphs using GraphPad Prism version 9.0.0
219 (GraphPad, USA).

220 **IS transposition analysis**

221 Sequences of the different IS elements encoded by *M. smegmatis* genome were obtained from
222 ISFinder database (26). ISMapper (27) was used to map out the different IS integration sites in
223 raw sequence reads of each sequenced D29-resistant mutant. Briefly, paired end Illumina reads
224 of a D29-resistant mutant, a FASTA file of the IS query sequence and a genbank file of the
225 reference genome (*M. smegmatis* mc^2 155, NCBI accession number CP000480.1) were used as

226 input files. The paired end Illumina reads were mapped to the IS query sequence using BWA-
227 MEM (28), which generates a SAM file as output. Sequences directly flanking the IS query (i.e.
228 pairs of unmapped reads that mapped to the end of the IS query sequence) as well as soft clipped
229 regions (reads containing sequences that mapped to the IS query and extend into neighboring
230 sequence) were extracted from the SAM file using SAMtools (29) and SAMBLASTER (30)
231 respectively. The extracted sequences were converted to FASTQ format using BEDTools (31)
232 and filtered using BioPython to extract soft clipped read portions that are 5-30 bp in length. The
233 resulting sequences were sorted into left and right flanking sequences and separately mapped to
234 the reference genome using BWA-MEM, and BEDTools was used to determine the exact
235 position of IS integration in the D29-resistant mutant. All detected IS integrations were verified
236 by PCR.

237 **Promoter reporter assay**

238 **Lawn appearance**

239 Strains were grown in 7H9 medium to OD_{600} 0.8-1, then diluted to OD_{600} 0.6. Ten microliters
240 from diluted culture of each strain was streaked on a plain 7H10 plate. The plate was dried and
241 incubated at 37 ^{o}C until appearance of clear bacterial lawn.

242 **Live fluorescence**

243 Strains were grown in 7H9 medium to OD_{600} 0.8-1, then diluted to OD_{600} 0.6. Two-fold serial
244 dilutions of the diluted cultures were prepared in triplicates for each strain in a 96-well
245 microplate to obtain OD_{600} 0.6, 0.3, 0.15, 0.075, 0.0375 and 0.01875. Fluorescence was
246 quantified in FlexStation 3 Multi-Mode Microplate Reader (Molecular Devices, USA) at
247 excitation and emission wavelengths of 488 nm and 520 nm respectively. Quantification data for
248 fluorescent strains were normalized by subtracting Ms^{Wt} fluorescence from that of each strain,
249 and the results were plotted as bar graphs in GraphPad Prism.

250 **Flow cytometry**

251 Flow cytometry was carried out as previously described (32) with modification. The strains were
252 grown in 7H9 medium to OD_{600} 0.8-1. Two milliliters of each strain was pelleted, washed twice
253 in PBS-Tween 80, and fixed in 1 mL of 4 % glutaraldehyde in PBS-Tween 80 at room

254 temperature for 30 minutes. The fixed cells were pelleted, re-suspended in 2 mL of sterile PBS,
255 and passed through a 40 µm filter prior to flow cytometry using a CytoFLEX flow cytometer
256 (Beckman Coulter, USA). A minimum of 10,000 cells were selected to count in focus GFP
257 events for each strain. Flow cytometry data was analyzed using FlowJo version 10.8.1.

258 **Confocal microscopy**

259 Strains were grown in 7H9 medium to OD_{600} 0.8-1. One milliliter of each strain was pelleted and
260 washed twice in PBS-Tween 80. The supernatant was discarded, the cells were re-suspended in 1
261 mL of 4 % glutaraldehyde in PBS-Tween 80 and allowed to stand at room temperature for 30
262 minutes. The fixed cells were pelleted and re-suspended in 200 µL of PBS-Tween 80. For each
263 strain, 5 µL of re-suspended fixed cells as well as a 10-fold serial dilution were mounted on a
264 microscope slide and covered with a coverslip, then observed under a Zeiss LSM 800 Confocal
265 Laser Scanning Microscope (Zeiss, Germany).

266 **Drug susceptibility testing (DST)**

267 Drug susceptibility testing was carried out by broth microdilution. Bacterial strains were cultured
268 in 7H9 medium at 37 ºC with shaking until OD_{600} 0.8-1, then diluted to a cell density of 10^5
269 colony forming units per milliliter (CFU/mL) in 7H9 without Tween 80. Bacterial cultures in
270 two-fold serial dilutions of each drug as well as a plain control were prepared in 96-well
271 microplates. The plates were incubated at 37 ºC for 3 – 5 days. Minimum inhibitory
272 concentration (MIC) was defined as the concentration at which visible bacterial growth was
273 inhibited.

274

275

276

277

278

279

280

281

Results

Spontaneous D29 resistance in *M. smegmatis*

We screened 137 colonies of *M. smegmatis* for D29 resistance after multiple cycles of exposure, and a vast majority of them (82.5 %, n = 113) were classified as D29-resistant isolates. We then selected and purified 24 colonies, re-screened them for D29 resistance and sequenced their genomes. Of these 24 isolates, two strains, A72.1 and 2.6.1, particularly stand out for their high level of resistance to D29. Both strains appear to manifest no obvious change in surface morphology, but exhibit high level of resistance when screened by spot-kill and plaque assays (Figure 1A, B), which suggests impaired D29 infection efficiency against A72.1 and 2.6.1. Notably, greater susceptibility is seen at higher D29 concentration (Figure 1A), possibly suggesting dose-dependent resistance. Phage adsorption assay indicates little to no effect on D29 adsorption to both strains, suggesting that the mechanism of resistance in both strains occurs at stage(s) beyond phage adsorption (Figure 1C). The D29-resistant mutants A72.1 and 2.6.1 sustained point mutations and two IS transposition events each, including IS6120 integration directly upstream of *mpr* in both mutants.

D29 infection triggers IS rearrangements in *M. smegmatis*

It is likely that other genetic factors alone or in combination with the identified mutations may be responsible for D29 resistance phenotypes of the mutants (20). For this reason, we carried out IS transposition analysis on raw FASTQ data obtained for each of the mutants as well as Ms^{Wt}. We first collected the sequences of all known IS elements encoded by the *M. smegmatis* genome from ISFinder database (26) and determined their prevalence across the genome (Table S1, Figure S1). We then identified all IS rearrangements that were present in the mutants but not in Ms^{Wt}, then verified them by PCR alongside the Ms^{Wt} control (Figure 2).

A total of 10 IS transposition events were detected in seven D29-resistant mutants, where 4 mutants had single event each and 3 had double. There had been six IS6120, three ISMsm1 and one IS1096 transposition events in the mutants, in which the IS integrations took place in six coding and three non-coding regions. A72.1 and 2.6.1 – the two strains that manifested incredibly higher level of D29 resistance compared to the other mutants – appear to have sustained two IS transposition events each, making them strains of particular interest (Figure 3).

311 Details about the integration position and protein products of the affected genes are outlined in
312 Table S2.

313 **A72.1 and 2.6.1 show elevated Mpr expression**

314 The two mutants A72.1 and 2.6.1 sustained two transposition events each. ISMsm1 integrated in
315 the intergenic region between *MSMEG_2105* and *MSMEG_2104* in A72.1, but integrated in
316 *MSMEG_5393* in 2.6.1. However, in both strains, IS6120 integrated within the 168 bp intergenic
317 region between *mpr* and *MSMEG_1237*, just upstream of *mpr*. Mpr-MSMEG_1237 interaction
318 map on STRING database suggests possible co-expression (Figure 4A). We therefore quantified
319 the expression of *mpr* and *MSMEG_1237* to determine if any of the genes had been affected by
320 IS6120 integration, using Ms^{Wt} and B6.1 as control strains. Both A72.1 and 2.6.1 appear to
321 manifest highly elevated Mpr expression, whereas *MSMEG_1237* expression remained similar
322 among the strains (Figure 4B). We also simultaneously quantified mRNA levels at the 168 bp
323 intergenic region (*MSGEG_1236-1237IR*) in both A72.1 and 2.6.1 as well as the control strains
324 to detect any variations. The mRNA levels at this region don't seem to differ much, and identical
325 DNA sizes were seen on agarose gel for the four strains after qPCR amplification (data not
326 shown).

327 **IS6120 integration upstream of *mpr* introduces a putative transcription factor-binding site**
328 **(TFBS) and a canonical -35 promoter element**

329 There is a 168 bp region between *mpr* and *MSMEG_1237*, and integration of IS6120 at this
330 region appears to primarily affect the expression of *mpr*, not *MSMEG_1237* (Figure 4). In
331 addition, IS6120 has the same orientation as *mpr* at the integration site, which raises the question
332 of whether IS6120 integration has had some regulatory influence over *mpr*. One way this could
333 happen is by promoter reconstitution, which inspired us to analyze the intergenic sequence prior
334 to IS6120 integration (or wild type sequence, *wtseq*) and that after integration (or reconstituted
335 sequence, *rcseq*) for possible presence of new promoter/regulatory element(s). We used four
336 promoter prediction programs, and each predicted at least one complete promoter in *rcseq*. One
337 program, Sima70Pred, predicted three promoters in *wtseq* and fourteen in *rcseq*, but the
338 remaining programs predicted no promoters in *wtseq* (Table S3). All promoters predicted by all
339 programs in *rcseq* have the sequence "**TTGACAAT**TCCTCgtcccgagttgtacgtt" in common,
340 which contains a putative TFBS for leucine-responsive regulatory protein (Lrp) as well as -35

341 and -10 promoter elements (Figure 5). The TFBS and the canonical -35 promoter element were
342 introduced at the site by IS6120 integration, implying that integration of IS6120 at the site
343 brought in these two elements to reconstitute a more complete promoter than that in *wtseq*.

344 **IS6120 integration reconstitutes a stronger promoter upstream of *mpr***

345 To verify the activity of the reconstituted promoter (*rcp*), we carried out GFP reporter assays by
346 constructing GFP-overexpressing strains using *rcp* or *wtp* (wild type promoter). We constructed
347 $Ms^{wtp\text{-}GFP}$ by transforming Ms^{Wt} with pMV-*wtp*-GFP, a GFP overexpression vector in which
348 *hsp60* promoter was replaced by *wtp* (the entire 168 bp region between *mpr* and *MSMEG_1237*,
349 amplified from Ms^{Wt}). Similarly, we constructed $Ms^{rcp\text{-}GFP}$ in which the *hsp60* promoter was
350 replaced by *rcp* (a region of equal length directly upstream of *mpr*, amplified from A72.1).
351 Ms^{GFP}, a strain overexpressing GFP from the *hsp60* promoter, was used as a control.

352 The first evidence of promoter activity manifested at colony level after transformation of bacteria
353 with the respective vectors. Ms^{GFP} and $Ms^{rcp\text{-}GFP}$ colonies manifested the characteristic green
354 color of GFP. Lawn of $Ms^{rcp\text{-}GFP}$ also shows the characteristic green coloration on plain 7H10
355 plates (Figure 6A). Though $Ms^{rcp\text{-}GFP}$ produces lower live fluorescence than Ms^{GFP}, it produces
356 far greater fluorescence than $Ms^{wtp\text{-}GFP}$, suggesting that introduction of the new elements by
357 IS6120 significantly increased the strength of the promoter at the integration site (Figure 6B).
358 We also counted GFP events for each of the strains by flow cytometry, and the number of GFP
359 events detected for $Ms^{rcp\text{-}GFP}$ was clearly far greater than that for $Ms^{wtp\text{-}GFP}$, which constitutes
360 further evidence of superior promoter activity (Figure 7). Finally, confocal micrographs
361 corroborate the flow cytometry data, showing that *wtp* drives significantly lower GFP expression
362 than *rcp*, and that the GFP signals produced by $Ms^{rcp\text{-}GFP}$ and Ms^{GFP} are somewhat identical
363 (Figure 8). Collectively, these imply that IS6120 integration upstream of *mpr* brings about
364 replacement of *wtp* by *rcp*, which raises the question of whether *M. smegmatis* regulates the
365 expression of Mpr by promoter reconstitution. In addition, we attempted to overexpress Mpr in
366 Ms^{Wt} by constructing $Ms^{wtp\text{-}Mpr}$ and $Ms^{rcp\text{-}Mpr}$ using the vectors pMV-*wtp-mpr* or pMV-*rcp-mpr*
367 respectively. However, strains transformed with pMV-*rcp-mpr* rarely formed colonies on the
368 plate (Figure S2). Due to low efficiency of $Ms^{rcp\text{-}Mpr}$ to form colonies, we are unable to provide
369 any definitive inference *vis-à-vis* the relationship between *rcp* and Mpr expression or D29

370 resistance. However, it does appear like expressing Mpr using *rcp* exerts toxicity on the bacterial
371 cells.

372

373 **D29 resistance had no effect on *M. smegmatis* resistance to selected drugs**

374 To assess potential fitness tradeoffs associated with D29 resistance, we performed drug
375 susceptibility testing (DST) on Ms^{Wt} and three resistant mutants (B6.1, A72.1, 2.6.1) against
376 seven frontline anti-tubercular agents: isoniazid, rifampicin, linezolid, clofazimine, bedaquiline,
377 levofloxacin, and ethambutol. Remarkably, all strains—including the resistant mutants—
378 exhibited identical susceptibility profiles to these antibiotics (Table S4). This lack of divergence
379 suggests that D29 resistance does not impinge upon core cellular processes targeted by these
380 drugs, nor does it incur detectable collateral costs in tolerance to these drugs. These findings
381 imply that mycobacterial adaptation to phage pressure may occur independently of classical
382 antibiotic resistance pathways.

383

384

385

386

387

388

389

390

391

392

393

394

395 **Discussion**

396 AMR triggered a renewed interest in phage therapy as a potential alternative to antibiotic therapy
397 (3,33,34). However, phage resistance represents a potent threat to sustainable usability of phage
398 therapy, addressing which would require dissecting the mechanisms of phage interactions with
399 their bacterial hosts. Efforts towards dissecting phage-bacteria interactions revealed invaluable
400 details regarding receptor requirements (19) and adaptive responses to phage pressure, including
401 the roles played by IS elements (20,42,43) as well as Mpr in M. smegmatis (15). Studies on Mpr
402 role in D29 resistance have relied on vector-borne overexpression of the gene. Here, we report
403 two D29-resistant mutants with elevated Mpr expression that likely stemmed from promoter
404 reconstitution by IS6120 integration directly upstream of *mpr*.

405 ISs are mobile genetic elements that are widespread in bacterial genomes and play important
406 roles in bacterial evolution and adaptation to stress. It is becoming increasingly evident that
407 phage infection triggers IS transposition, which causes these elements to integrate into certain
408 genes in bacteria and cause phage resistance via different mechanisms (20,42,43). For example,
409 TM4 infection of *M. smegmatis* triggers IS1096 transposition and integration into *lsr2*, hence
410 activating the LOS cluster, causing PIMs accumulation and reduced phage adsorption (20). Such
411 transposition events often cause large insertions that, coupled with widespread endogenous
412 presence of IS elements in the chromosome, may often be missed by mere SNP calling. This
413 explains why they were not detected during the initial whole-genome sequence analysis.
414 Therefore, we analyzed the raw sequence data for all sequenced D29-resistant mutants using
415 ISMapper (27), and we detected several IS transposition events (Figure 3A). We investigated one
416 particular transposition event in A72.1 and 2.6.1, which resulted in integration of IS6120 within
417 the 168 bp region between *MSMEG_1236* (multi-copy phage resistance gene, *mpr*) and
418 *MSMEG_1237* (Figure 3B). Mpr is a membrane-bound DNA exonuclease that, upon
419 overexpression, defends *M. smegmatis* against D29 by cleaving phage DNA following its
420 injection into the cytoplasm (14–16).

421 Mpr is required for the emergence of spontaneous D29-resistant mutants, and such role does not
422 require any mutation in the gene but overexpression of the wild type gene. However, the genetic
423 basis for emergence of D29-resistant mutants with elevated Mpr expression remained elusive.
424 Here, we uncovered that both A72.1 and 2.6.1 have IS6120 integration directly upstream of *mpr*,

425 and both show profoundly elevated expression of Mpr, not MSMEG_1237 (Figure 4B). In
426 addition, the integrated IS6120 element runs in the same orientation (5'-3') as *mpr*, not
427 *MSMEG_1237*, which could partly explain the IS transposition effect on Mpr rather than
428 MSMEG_1237. Further analysis of the sequence at the integration site revealed that IS6120
429 introduced a -35 promoter element and a TFBS for Lrp, which were not originally present at the
430 site, hence reconstituting a new, fuller promoter (Figure 5). Promoter reporter assays reveal that
431 the reconstituted promoter (*rcp*) has activity that is far superior than that of the original promoter
432 (*wtp*) and is nearly as good as the BCG promoter *hsp60* (Figures 7 and 8). This certainly begs the
433 question of whether elevated Mpr expression in spontaneous D29-resistant mutants has always
434 been due to reconstitution of a fuller, more powerful promoter upstream of *mpr*, which may also
435 explain why emergence of such mutants require the presence of an intact *mpr* (15). Failure to
436 isolate recombinant strains overexpressing *rcp-mpr* suggest extreme toxicity, and this is
437 consistent with previous effort to express *mpr* in *M. smegmatis* using the *hsp60* promoter (14).
438 This mechanism of gene regulation by promoter reconstitution is common in bacteria (44–46),
439 and the extreme toxicity may well be reminiscent of such situations where inherent protein
440 toxicity often makes it difficult to study (10,45). Mechanism of Mpr-mediated defense is
441 believed to be non-abortive in nature (16), and it remains to be seen whether A72.1 and 2.6.1
442 were able to grow normally in the face of elevated Mpr expression because the observed
443 expression levels were tolerable, or possibly due to neutralization of toxicity by other factors,
444 likely the second transposition event or other mutations detected in each of these strains. DEMs
445 of D29 have been reported for vector-borne Mpr-overexpressing *M. smegmatis* (16), but we were
446 unable to isolate a DEM for A72.1 and 2.6.1 in this study. It is not clear whether this could be
447 due to chromosome-borne, *rcp*-driven Mpr overexpression or absolute resistance in these strains
448 (13).

449 Mpr contains two major domains - a transmembrane domain (amino acids 33-50) and the domain
450 of unknown function DUF4352 (amino acids 83-211). DUF4352 is believed to be of viral origin,
451 suggesting that the bacteria likely acquired it during the course of evolution with viral predators,
452 then kept it for anti-viral defense (16). The fact that Ms^{Wt} is susceptible to D29 is evidence that
453 wild type level of Mpr expression does not confer resistance. However, regulation of Mpr
454 expression by promoter reconstitution could suggest that the gene is most useful to the bacteria

455 under D29-induced stress, not normal conditions. From our observations, Mpr appears to be the
456 primary anti-D29 resistance tool in *M. smegmatis*.

457 Events such as gene amplification-duplication are transient adaptive responses to increase
458 bacterial fitness, and are usually reversible due to the high fitness costs they exert (47,48). IS
459 transposition could also be reversible (43), but we haven't seen any evidence of such reversion in
460 A72.1 and 2.6.1 despite high expression of the toxic protein Mpr, and it remains to be seen
461 whether this might happen in later generations of the bacteria. Tolerance of A72.1 and 2.6.1 to
462 drugs appears to be unaffected, meaning that the strains had not traded off tolerance to the drugs
463 (at least those tested in this study) for D29 resistance. They also fare very well under normal
464 growth conditions, indicating lack of growth-related fitness cost associated with D29 resistance
465 in the strains.

466 This study reveals a form of gene regulation by promoter reconstitution in *M. smegmatis*. We
467 report that exposure of *M. smegmatis* to the lytic mycobacteriophage D29 triggers the
468 transposition and integration of IS6120 directly upstream of *mpr*, resulting in reconstitution of a
469 fuller, stronger promoter. This likely represents a previously elusive factor behind emergence of
470 D29-resistant mutants with elevated Mpr expression.

471 **Acknowledgments**

472 This study was supported by the National Key R&D Program of China (2021YFA1300900), the
473 Major Project of Guangzhou National Laboratory (GZNL2024A01009, GZNL2025C01003), the
474 National Natural Science Foundation of China (82502762).

475 **Data availability**

476 The next generation sequencing reads for Ms^{Wt}, 2.6.1 and A72.1 have been deposited at the
477 NCBI Sequence Read Archive, and can be accessed with SAMN55349604, SAMN55349605
478 and SAMN55349614 respectively.

479

480

481

482 **References**

483 1. GBD 2021 Antimicrobial Resistance Collaborators. Global burden of bacterial
484 antimicrobial resistance 1990-2021: a systematic analysis with forecasts to 2050. *Lancet.*
485 2024;404(10459):1199-1226. doi: 10.1016/S0140-6736(24)01867-1.
486 2. Expanded Access | FDA https://www.fda.gov/news-events/public-health-
487 focus/expanded-access
488 3. Dedrick RM, Guerrero-Bustamante CA, Garlena RA, Russell DA, Ford K, Harris K,
489 Gilmour KC, Soothill J, Jacobs-Sera D, Schooley RT, Hatfull GF, Spencer H. Engineered
490 bacteriophages for treatment of a patient with a disseminated drug-resistant
491 *Mycobacterium abscessus*. *Nat Med.* 2019; 25(5):730-733. doi: 10.1038/s41591-019-
492 0437-z.
493 4. Cristinziano M, Shashkina E, Chen L, Xiao J, Miller MB, Doligalski C, Coakley R, Lobo
494 LJ, Footer B, Bartelt L, Abad L, Russell DA, Garlena R, Lauer MJ, Viland M,
495 Kaganovsky A, Mowry E, Jacobs-Sera D, van Duin D, Kreiswirth BN, Hatfull GF,
496 Friedland A. Use of epigenetically modified bacteriophage and dual beta-lactams to treat
497 a *Mycobacterium abscessus* sternal wound infection. *Nat Commun.* 2024; 15(1):10360.
498 doi: 10.1038/s41467-024-54666-4.
499 5. Dedrick RM, Smith BE, Cristinziano M, Freeman KG, Jacobs-Sera D, Belessis Y,
500 Whitney Brown A, Cohen KA, Davidson RM, van Duin D, Gainey A, Garcia CB, Robert
501 George CR, Haidar G, Ip W, Iredell J, Khatami A, Little JS, Malmivaara K, McMullan
502 BJ, Michalik DE, Moscatelli A, Nick JA, Tupayachi Ortiz MG, Polenakovik HM,
503 Robinson PD, Skurnik M, Solomon DA, Soothill J, Spencer H, Wark P, Worth A,
504 Schooley RT, Benson CA, Hatfull GF. Phage Therapy of *Mycobacterium* Infections:
505 Compassionate Use of Phages in 20 Patients With Drug-Resistant Mycobacterial Disease.
506 *Clin Infect Dis.* 2023; 76(1):103-112. doi: 10.1093/cid/ciac453.
507 6. Dedrick RM, Freeman KG, Nguyen JA, Bahadirli-Talbott A, Smith BE, Wu AE, Ong AS,
508 Lin CT, Ruppel LC, Parrish NM, Hatfull GF, Cohen KA. Potent antibody-mediated
509 neutralization limits bacteriophage treatment of a pulmonary *Mycobacterium abscessus*
510 infection. *Nat Med.* 2021; 27(8):1357-1361. doi: 10.1038/s41591-021-01403-9.
511 7. Nick JA, Dedrick RM, Gray AL, Vladar EK, Smith BE, Freeman KG, Malcolm KC,
512 Epperson LE, Hasan NA, Hendrix J, Callahan K, Walton K, Vestal B, Wheeler E,

513 Rysavy NM, Poch K, Caceres S, Lovell VK, Hisert KB, de Moura VC, Chatterjee D, De
514 P, Weakly N, Martiniano SL, Lynch DA, Daley CL, Strong M, Jia F, Hatfull GF,
515 Davidson RM. Host and pathogen response to bacteriophage engineered against
516 *Mycobacterium abscessus* lung infection. *Cell.* 2022; 185(11):1860-1874.e12. doi:
517 10.1016/j.cell.2022.04.024.
518 8. Little JS, Dedrick RM, Freeman KG, Cristinziano M, Smith BE, Benson CA, Jhaveri TA,
519 Baden LR, Solomon DA, Hatfull GF. Bacteriophage treatment of disseminated cutaneous
520 *Mycobacterium chelonae* infection. *Nat Commun.* 2022; 13(1):2313. doi:
521 10.1038/s41467-022-29689-4.
522 9. Dedrick RM, Freeman KG, Nguyen JA, Bahadirli-Talbott A, Cardin ME, Cristinziano M,
523 Smith BE, Jeong S, Ignatius EH, Lin CT, Cohen KA, Hatfull GF. Nebulized
524 Bacteriophage in a Patient With Refractory *Mycobacterium abscessus* Lung Disease.
525 *Open Forum Infect Dis.* 2022; 9(7):ofac194. doi: 10.1093/ofid/ofac194.
526 10. Dedrick RM, Jacobs-Sera D, Bustamante CA, Garlena RA, Mavrich TN, Pope WH,
527 Reyes JC, Russell DA, Adair T, Alvey R, Bonilla JA, Bricker JS, Brown BR, Byrnes D,
528 Cresawn SG, Davis WB, Dickson LA, Edgington NP, Findley AM, Golebiewska U,
529 Grose JH, Hayes CF, Hughes LE, Hutchison KW, Isern S, Johnson AA, Kenna MA,
530 Klyczek KK, Mageeney CM, Michael SF, Molloy SD, Montgomery MT, Neitzel J, Page
531 ST, Pizzorno MC, Poxleitner MK, Rinehart CA, Robinson CJ, Rubin MR, Teyim JN,
532 Vazquez E, Ware VC, Washington J, Hatfull GF. Prophage-mediated defence against
533 viral attack and viral counter-defence. *Nat Microbiol.* 2017; 2:16251. doi:
534 10.1038/nmicrobiol.2016.251.
535 11. Mageeney CM, Mohammed HT, Dies M, Anbari S, Cudkevich N, Chen Y, Buceta J,
536 Ware VC. *Mycobacterium* Phage Butters-Encoded Proteins Contribute to Host Defense
537 against Viral Attack. *mSystems.* 2020; 5(5):e00534-20. doi: 10.1128/mSystems.00534-20.
538 12. Gentile GM, Wetzel KS, Dedrick RM, Montgomery MT, Garlena RA, Jacobs-Sera D,
539 Hatfull GF. More Evidence of Collusion: a New Prophage-Mediated Viral Defense
540 System Encoded by Mycobacteriophage Sbash. *mBio.* 2019; 10(2):e00196-19. doi:
541 10.1128/mBio.00196-19.
542 13. Mohammed HT, Mageeney C, Ware VC. Identification of a new antiphage system in
543 *Mycobacterium* phage Butters.

544 *bioRxiv* 2023.01.03.522681; doi: https://doi.org/10.1101/2023.01.03.522681
545 14. Barsom EK, Hatfull GF. Characterization of *Mycobacterium smegmatis* gene that confers
546 resistance to phages L5 and D29 when overexpressed. *Mol Microbiol.* 1996; 21(1):159-
547 70. doi: 10.1046/j.1365-2958.1996.6291342.x.
548 15. Seniya SP, Jain V. Decoding phage resistance by *mpr* and its role in survivability of
549 *Mycobacterium smegmatis*. *Nucleic Acids Res.* 2022; 50(12):6938-6952. doi:
550 10.1093/nar/gkac505.
551 16. Sharma S, Jain V. Structural and functional relevance of the DUF4352 domain in
552 antiviral immunity and physiology of mycobacteria. *Nucleic Acids Res.*
553 2025;53(20):gkaf1253. doi: 10.1093/nar/gkaf1253.
554 17. Huang Y, Xu H, Zhang T, Liao Y, Hu J, Huang Z, Hu H, Li P, Fan L, Xie J.
555 Mycobacterial non-homologous end joining is required for antiphage defense. *Nucleic*
556 *Acids Res.* 2026;54(3):gkag066. doi: 10.1093/nar/gkag066.
557 18. Sørensen PE, Baig S, Stegger M, Ingmer H, Garmyn A, Butaye P. Spontaneous Phage
558 Resistance in Avian Pathogenic *Escherichia coli*. *Front Microbiol.* 2021;12:782757. doi:
559 10.3389/fmicb.2021.782757.
560 19. McKitterick AC, Bernhardt TG. Phage resistance profiling identifies new genes required
561 for biogenesis and modification of the corynebacterial cell envelope. *Elife.*
562 2022;11:e79981. doi: 10.7554/eLife.79981.
563 20. Li Y, Wei Y, Guo X, Li X, Lu L, Hu L, He ZG. Insertion sequence transposition activates
564 antimycobacteriophage immunity through an *lsr2*-silenced lipid metabolism gene island.
565 *mLife.* 2024; 3(1):87-100. doi: 10.1002/mlf2.12106.
566 21. Wilson K. Preparation of genomic DNA from bacteria. *Curr Protoc Mol Biol.*
567 2001;Chapter 2:Unit 2.4. doi: 10.1002/0471142727.mb0204s56.
568 22. Afgan E, Baker D, Batut B, van den Beek M, Bouvier D, Cech M, Chilton J, Clements D,
569 Coraor N, Grüning BA, Guerler A, Hillman-Jackson J, Hiltemann S, Jalili V, Rasche H,
570 Soranzo N, Goecks J, Taylor J, Nekrutenko A, Blankenberg D. The Galaxy platform for
571 accessible, reproducible and collaborative biomedical analyses: 2018 update. *Nucleic*
572 *Acids Res.* 2018;46(W1):W537-W544. doi: 10.1093/nar/gky379.
573 23. Andrews S. (2010). FastQC: A quality control tool for high throughput sequence data.
574 Available online at https://www.bioinformatics.babraham.ac.uk/projects/fastqc/

575 24. Chen S, Zhou Y, Chen Y, Gu J. fastp: an ultra-fast all-in-one FASTQ preprocessor.
576 *Bioinformatics.* 2018;34(17):i884-i890. doi: 10.1093/bioinformatics/bty560.
577 25. Seemann T (2015) snippy: fast bacterial variant calling from NGS reads Available online
578 at https://github.com/tseemann/snippy
579 26. Siguier P, Perochon J, Lestrade L, Mahillon J, Chandler M. ISfinder: the reference centre
580 for bacterial insertion sequences. *Nucleic Acids Res.* 2006;34(Database issue):D32-6. doi:
581 10.1093/nar/gkj014.
582 27. Hawkey J, Hamidian M, Wick RR, Edwards DJ, Billman-Jacobe H, Hall RM, Holt KE.
583 ISMapper: identifying transposase insertion sites in bacterial genomes from short read
584 sequence data. *BMC Genomics.* 2015;16(1):667. doi: 10.1186/s12864-015-1860-2.
585 28. Li H, Durbin R. Fast and accurate short read alignment with Burrows-Wheeler transform.
586 *Bioinformatics.* 2009;25(14):1754-60. doi: 10.1093/bioinformatics/btp324.
587 29. Li H, Handsaker B, Wysoker A, Fennell T, Ruan J, Homer N, Marth G, Abecasis G,
588 Durbin R; 1000 Genome Project Data Processing Subgroup. The Sequence
589 Alignment/Map format and SAMtools. *Bioinformatics.* 2009;25(16):2078-9. doi:
590 10.1093/bioinformatics/btp352.
591 30. Faust GG, Hall IM. SAMBLASTER: fast duplicate marking and structural variant read
592 extraction. *Bioinformatics.* 2014;30(17):2503-5. doi: 10.1093/bioinformatics/btu314.
593 31. Quinlan AR, Hall IM. BEDTools: a flexible suite of utilities for comparing genomic
594 features. *Bioinformatics.* 2010;26(6):841-2. doi: 10.1093/bioinformatics/btq033.
595 32. Kriel NL, Newton-Foot M, Bennion OT, Aldridge BB, Mehaffy C, Belisle JT, Walzl G,
596 Warren RM, Sampson SL, Gey van Pittius NC. Localization of $EccA_3$ at the growing
597 pole in *Mycobacterium smegmatis*. *BMC Microbiol.* 2022;22(1):140. doi:
598 10.1186/s12866-022-02554-6.
599 33. Schooley RT, Biswas B, Gill JJ, Hernandez-Morales A, Lancaster J, Lessor L, Barr JJ,
600 Reed SL, Rohwer F, Benler S, Segall AM, Taplitz R, Smith DM, Kerr K, Kumaraswamy
601 M, Nizet V, Lin L, McCauley MD, Strathdee SA, Benson CA, Pope RK, Leroux BM,
602 Picel AC, Mateczun AJ, Cilwa KE, Regeimbal JM, Estrella LA, Wolfe DM, Henry MS,
603 Quinones J, Salka S, Bishop-Lilly KA, Young R, Hamilton T. Development and Use of
604 Personalized Bacteriophage-Based Therapeutic Cocktails To Treat a Patient with a
605 Disseminated Resistant *Acinetobacter baumannii* Infection. *Antimicrob Agents*

606 *Chemother.* 2017;61(10):e00954-17. doi: 10.1128/AAC.00954-17.
607 34. Aslam S, Courtwright AM, Koval C, Lehman SM, Morales S, Furr CL, Rosas F,
608 Brownstein MJ, Fackler JR, Sisson BM, Biswas B, Henry M, Luu T, Bivens BN,
609 Hamilton T, Duplessis C, Logan C, Law N, Yung G, Turowski J, Anesi J, Strathdee SA,
610 Schooley RT. Early clinical experience of bacteriophage therapy in 3 lung transplant
611 recipients. *Am J Transplant.* 2019;19(9):2631-2639. doi: 10.1111/ajt.15503.
612 35. Besra GS, Khoo KH, Belisle JT, McNeil MR, Morris HR, Dell A, Brennan PJ. New
613 pyruvylated, glycosylated acyltrehaloses from *Mycobacterium smegmatis* strains, and
614 their implications for phage resistance in mycobacteria. *Carbohydr Res.* 1994;251:99-114.
615 doi: 10.1016/0008-6215(94)84279-5.
616 36. Dhariwal KR, Liav A, Vatter AE, Dhariwal G, Goren MB. Haptenic oligosaccharides in
617 antigenic variants of mycobacterial C-mycosides antagonize lipid receptor activity for
618 mycobacteriophage D4 by masking a methylated rhamnose. *J Bacteriol.*
619 1986;168(1):283-93. doi: 10.1128/jb.168.1.283-293.1986.
620 37. Furuchi A, Tokunaga T. Nature of the receptor substance of *Mycobacterium smegmatis*
621 for D4 bacteriophage adsorption. *J Bacteriol.* 1972;111(2):404-11. doi:
622 10.1128/jb.111.2.404-411.1972.
623 38. Imaeda T, Blas FS. Adsorption of Mycobacteriophage on Cell-wall Components. *J Gen*
624 *Virol.* 1969;5(4):493–8.
625 39. Wetzel KS, Illouz M, Abad L, Aull HG, Russell DA, Garlena RA, Cristinziano M,
626 Malmsheimer S, Chalut C, Hatfull GF, Kremer L. Therapeutically useful
627 mycobacteriophages BPs and Muddy require trehalose polyphleates. *Nat Microbiol.*
628 2023;8(9):1717-1731. doi: 10.1038/s41564-023-01451-6.
629 40. Li X, Long X, Chen L, Guo X, Lu L, Hu L, He ZG. Mycobacterial phage TM4 requires a
630 eukaryotic-like Ser/Thr protein kinase to silence and escape anti-phage immunity. *Cell*
631 *Host Microbe.* 2023;31(9):1469-1480.e4. doi: 10.1016/j.chom.2023.07.005.
632 41. Chen J, Kriakov J, Singh A, Jacobs WR, Besra GS, Bhatt A. Defects in glycopeptidolipid
633 biosynthesis confer phage I3 resistance in *Mycobacterium smegmatis*. *Microbiology*
634 *(Reading).* 2009;155(Pt 12):4050-4057. doi: 10.1099/mic.0.033209-0.
635 42. Fujiki J, Nakamura T, Kreimeyer H, Llorente C, Fouts DE, Schnabl B. Insertion
636 sequence-mediated phage resistance contributes to attenuated colonization of

637 cytolytic *Enterococcus faecalis* variants in the gut. *Microbiol Spectr.*
638 2025;13(5):e0330324. doi: 10.1128/spectrum.03303-24.
639 43. Styles KM, Locke RK, Cowley LA, Brown AT, Sagona AP. Transposable Element
640 Insertions into the *Escherichia coli* Polysialic Acid Gene Cluster Result in Resistance to
641 the K1F Bacteriophage. *Microbiol Spectr.* 2022;10(3):e0211221. doi:
642 10.1128/spectrum.02112-21.
643 44. Durrant MG, Perry NT, Pai JJ, Jangid AR, Athukoralage JS, Hiraizumi M, McSpedon JP,
644 Pawluk A, Nishimasu H, Konermann S, Hsu PD. Bridge RNAs direct programmable
645 recombination of target and donor DNA. *Nature.* 2024;630(8018):984-993. doi:
646 10.1038/s41586-024-07552-4.
647 45. Wilkinson ME, Li D, Gao A, Macrae RK, Zhang F. Phage-triggered reverse transcription
648 assembles a toxic repetitive gene from a noncoding RNA. *Science.*
649 2024;386(6717):eadq3977. doi: 10.1126/science.adq3977.
650 46. Ton-Hoang B, Bétermier M, Polard P, Chandler M. Assembly of a strong promoter
651 following IS911 circularization and the role of circles in transposition. *EMBO J.*
652 1997;16(11):3357-71. doi: 10.1093/emboj/16.11.3357.
653 47. Andersson DI, Hughes D. Gene amplification and adaptive evolution in bacteria. *Annu*
654 *Rev Genet.* 2009;43:167-95. doi: 10.1146/annurev-genet-102108-134805.
655 48. Kugelberg E, Kofoid E, Reams AB, Andersson DI, Roth JR. Multiple pathways of
656 selected gene amplification during adaptive mutation. *Proc Natl Acad Sci U S A.*
657 2006;103(46):17319-24. doi: 10.1073/pnas.0608309103.

658

659

660

661

662

663

664

665

666 **Tables and Figure Legends**

667

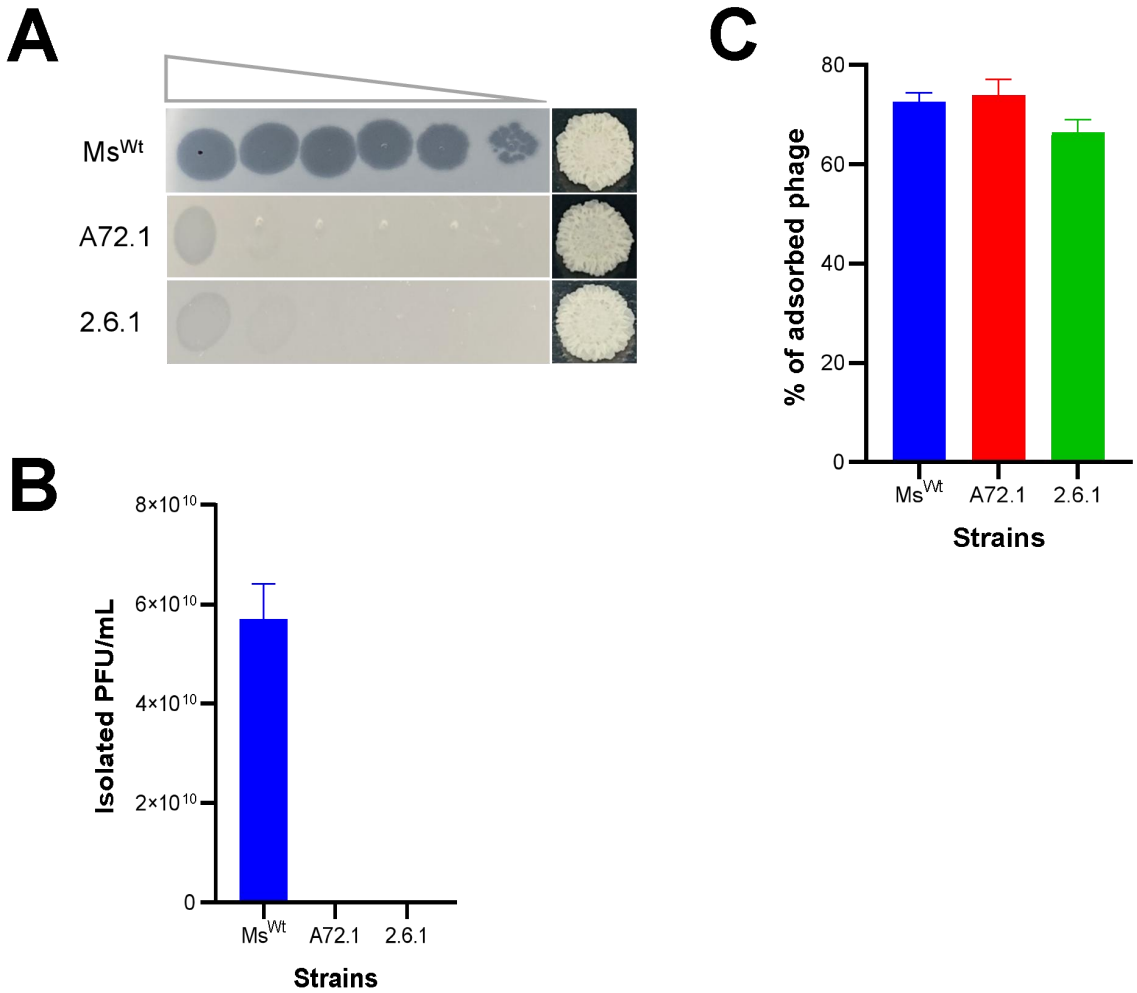

668
669 **Figure 1 Spontaneous D29 resistance in *M. smegmatis.*** A, A72.1 and 2.6.1 were tested for D29 resistance by
670 spot-kill assay, and both appear to be particularly highly resistant to D29 compared to Ms^{Wt}. B, both strains
671 were also tested for D29 resistance by plaque assay, which appears to be consistent with the spot-kill assay. C,
672 terminal adsorption suggests that D29 adsorption is not inhibited in the two strains, suggesting that the
673 resistance mechanism is at a stage downstream of phage adsorption.

674

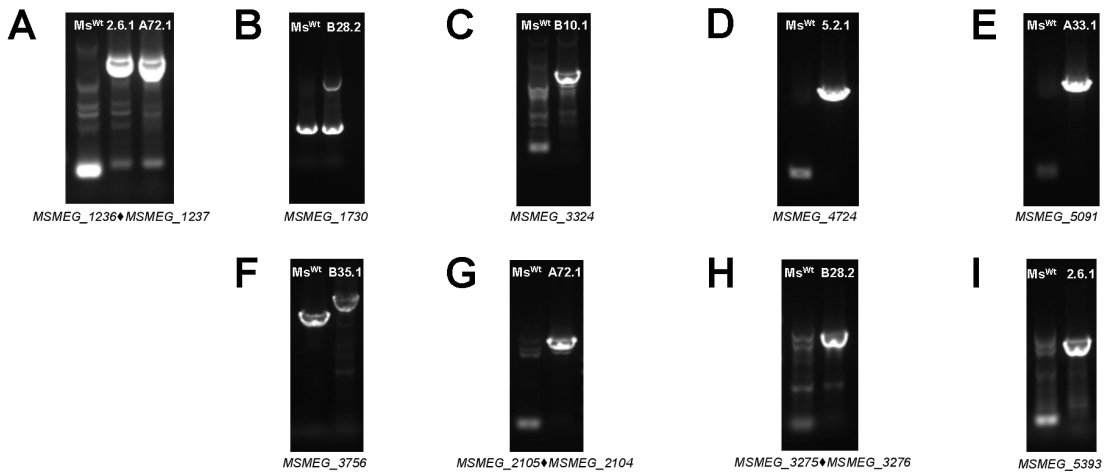

Panel		A	B	C	D	E	F	G	H	I
IS element		IS6120	IS6120	IS6120	IS6120	IS6120	IS1096	ISMsm1	ISMsm1	ISMsm1
Size (bp)	before	154	486	153	166	72	3169	134	79	141
	after	1631	1962	1629	1641	1547	5419	1475	1419	1482

675

676 **Figure 2 PCR verification of IS rearrangements.** A total of 7 (29.2 %) of the sequenced D29-resistant
677 mutants sustained at least a single IS transposition event. PCR verification of integration at each site as well as
678 affected gene/region are shown in the upper panels A-I, whereas sizes at the site before and after IS integration
679 are outlined in the lower table in the figure. Integration at intergenic region is indicated by a "black diamond
680 icon" between the two genes.

681

A

	A33.1	A72.1	B10.1	B28.2	B35.1	2.6.1	5.2.1
MSMEG_1236 ♦ MSMEG_1237		IS6120				IS6120	
MSMEG_1730				IS6120			
MSMEG_2105 ♦ MSMEG_2104		ISMsm1					
MSMEG_3275 ♦ MSMEG_3276				ISMsm1			
MSMEG_3324			IS6120				
MSMEG_3756 (rrlA)					IS1096		
MSMEG_4724							IS6120
MSMEG_5091	IS6120						
MSMEG_5393 (kdpB)						ISMsm1	

B

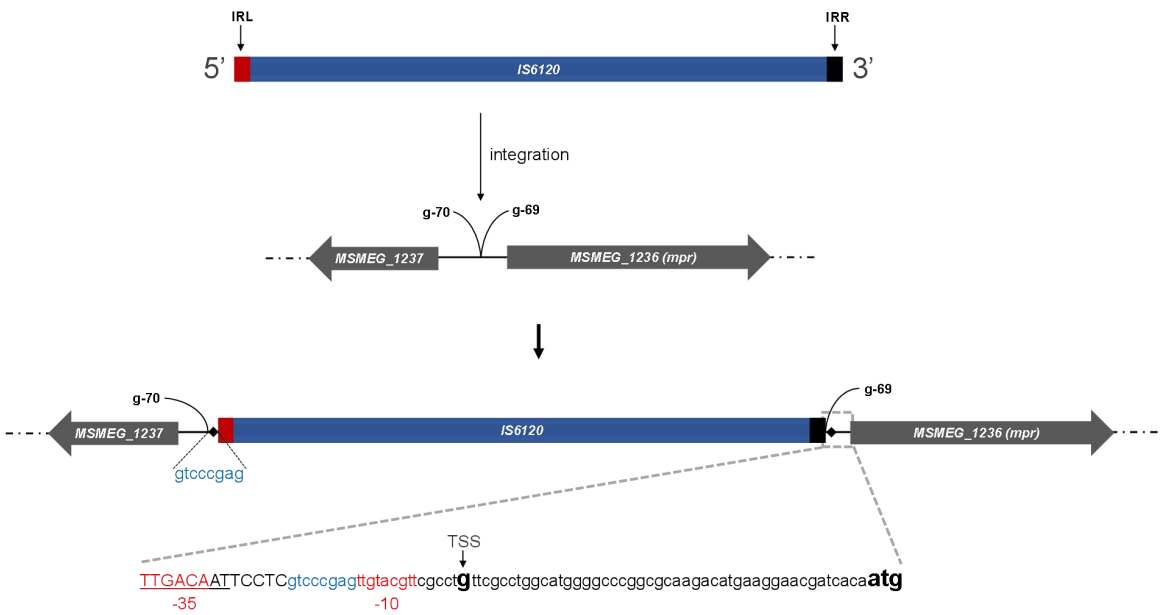

682

683 **Figure 3 IS rearrangements in the D29-resistant mutants.** A, the different strains/regions affected by IS
684 rearrangements. IS integration at intergenic region is indicated by a "black diamond" between the two genes. B,
685 both A72.1 and 2.6.1 – the D29-resistant mutants manifesting the highest level of resistance – sustained
686 IS6120 integration between nucleotides G-70 and G-69 upstream of *MSMEG_1236* (*mpr*). This integration
687 resulted in two direct repeats (indicated by black diamonds) at either sides of IS6120 at the integration site as
688 well as introduction of the -35 promoter element "TTGACA" and a transcription factor-binding site (TFBS)
689 for Lrp (leucine-responsive regulatory protein). Figure is drawn in a reverse orientation. Upper case letters,
690 nucleotides introduced by IS6120 integration; underlined letters, TFBs; lower case letters, original sequence at
691 the site; blue-font letters, direct repeats; TSS, transcription start site; atg, *mpr* start codon.

692

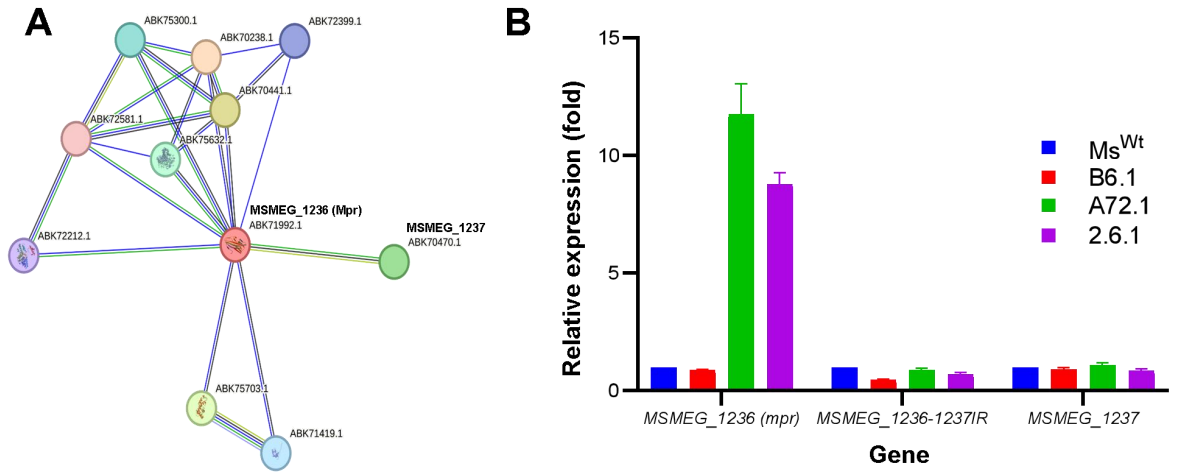

693

694 **Figure 4 Elevated Mpr expression in A72.1 and 2.6.1.** A, STRING protein-protein interaction network for
695 Mpr. Mpr and MSMEG_1237 are adjacent to each other, and a possible co-expression is predicted in their
696 interaction profile. B, RT-qPCR of Mpr, MSMEG_1237 as well as their intergenic region (IR) reveals that
697 Mpr expression is elevated in A72.1 and 2.6.1.

698

Number of predicted promoters in:

Prediction program	*wtseq*	*rcseq*
BPROM	0	1
BGDP	0	1
Sigma70Pred	3	14
PePPER	0	1

-35 -10

TTGACAATTCCTCgtcccgagttgtacgtt

TFBS

Upper case, IS6120 sequence
Lower case, original sequence

699

700 **Figure 5 Promoter prediction in *rcseq*.** Four promoter prediction programs detected the presence of a new
701 promoter in *rcseq*. All these promoters share one sequence in common, which contains a putative TFBS, -35
702 and -10 promoter elements.

703

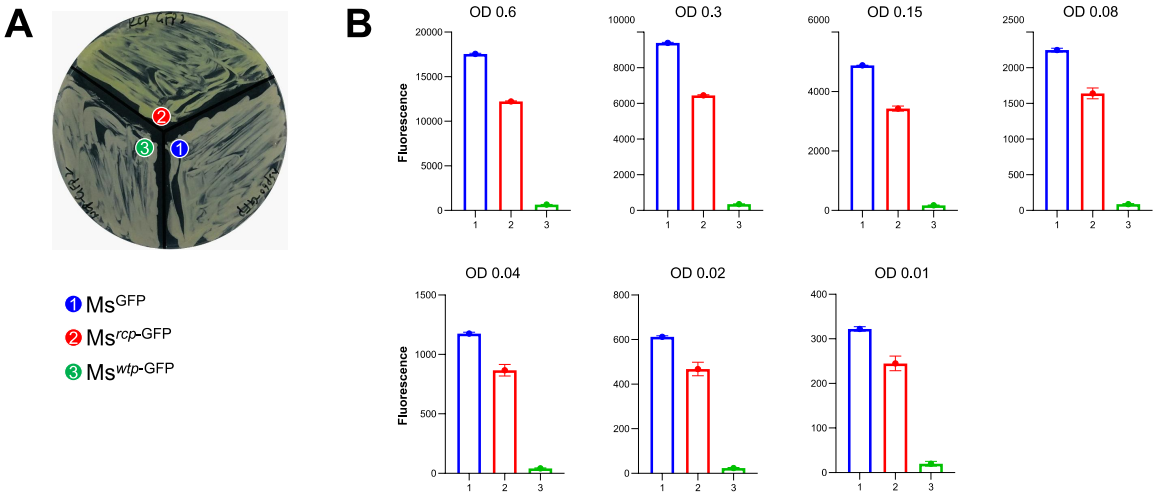

Figure 6 Quantification of *wtp*- and *rcp*-driven green fluorescence. A, Lawn appearance of GFP-expressing strains using *hsp60*, *wtp* and *rcp*. $Ms^{rcp\text{-}GFP}$ shows the characteristic green coloration of GFP. B, Live fluorescence of each strain as quantified using a microplate reader at different optical densities indicates that *rcp* drives higher fluorescence than *wtp*.

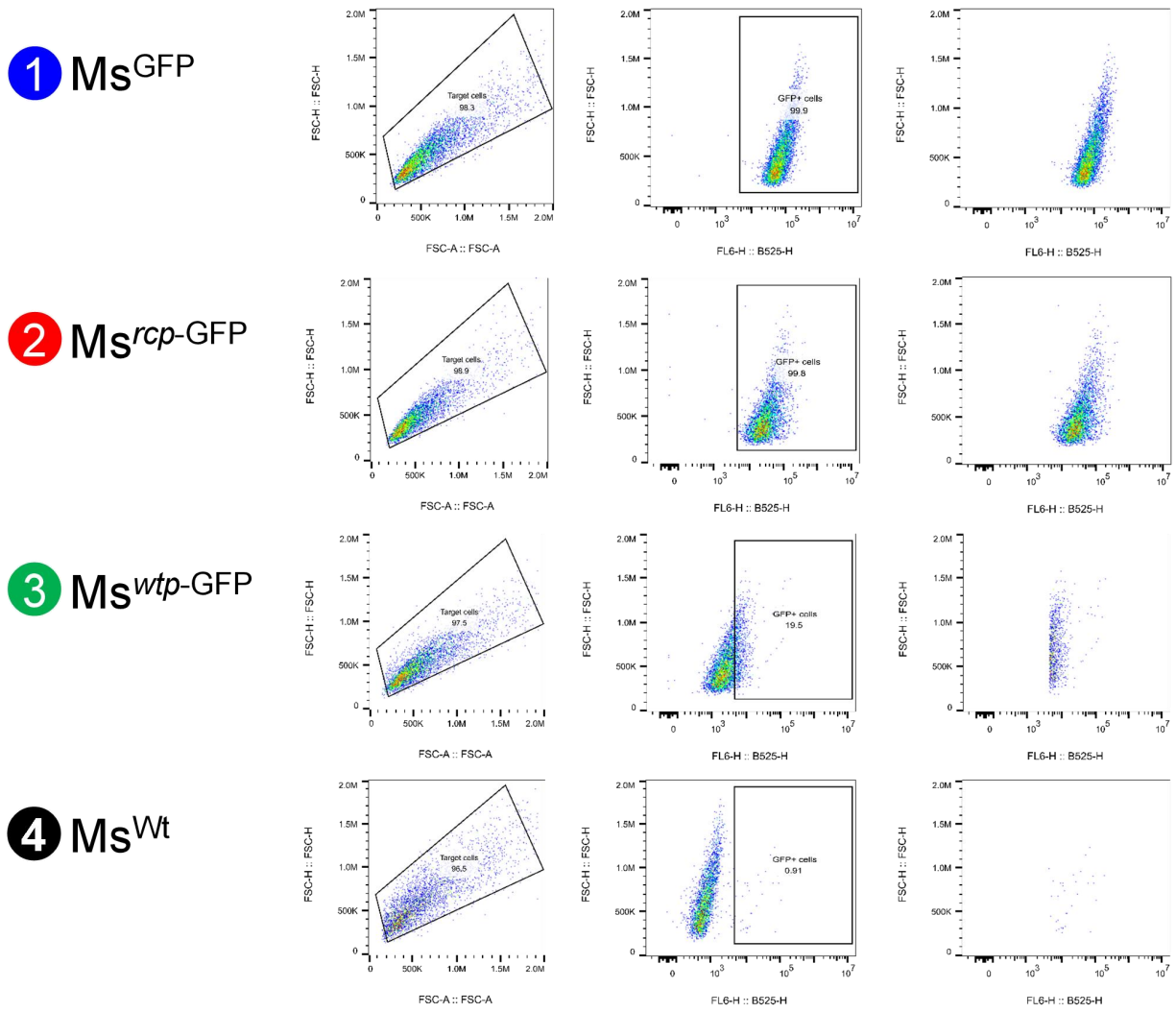

710

711 **Figure 7 Quantification of *wtp*- and *rcp*-driven GFP events by flow cytometry.** Quantification of GFP
712 events places *hsp60* and *rcp* on par with each other, whereas *wtp* falls far behind in comparison. Quantification
713 was carried out in a 10,000-cell population for each strain. Populations expressing GFP using *hsp60* (Ms^{GFP}),
714 *rcp* ($Ms^{rcp\text{-}GFP}$) and *wtp* ($Ms^{wtp\text{-}GFP}$) had 99.9, 99.8 and 19.5 % GFP-positive cells respectively. In contrast, the
715 negative control (Ms^{Wt} population) had a negligible 0.91 % GFP-false positive cells.

716

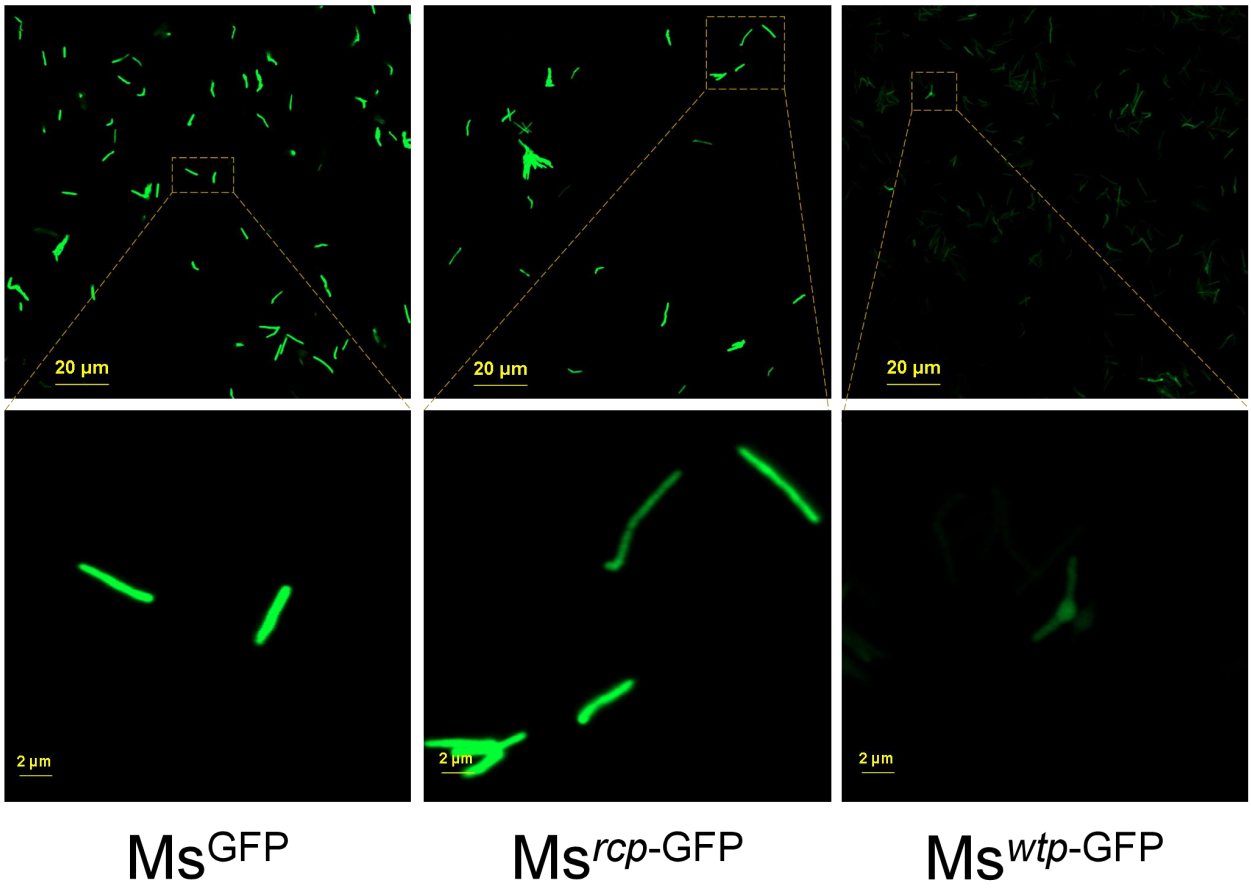

Figure 8 Quantification of fluorescence signal. Fluorescence signal driven by *hsp60*, *rcp* and *wtp* were quantified by confocal laser scanning microscopy. Strength of signal produced by *hsp60* and *rcp* appear to be similar, whereas *wtp* drives far weaker fluorescence signal under the microscope.